Environmental Science & Technology

pubs.acs.org/est

Article

Chloramination of Nitromethane: Incomplete Chlorination and Unexpected Substitution Reaction

Jiaming Lily Shi,[§] Euna Kim,[§] Georgia B. Cardosa, and Daniel L. McCurry*

Cite This: https://doi.org/10.1021/acs.est.2c09821

Read Online

ACCESS | Metrics & More | Article Recommendations | Supporting Information

ABSTRACT: Ozone is commonly used as a predisinfectant in potable water reuse treatment trains. Nitromethane was recently found as a ubiquitous ozone byproduct in wastewater, and the key intermediate toward chloropicrin during subsequent secondary disinfection of ozonated wastewater effluent with chlorine. However, many utilities have switched from free chlorine to chloramines as a secondary disinfectant. The reaction mechanism and kinetics of nitromethane transformation by chloramines, unlike those for free chlorine, are unknown. In this work, the kinetics, mechanism, and products of nitromethane chloramination were studied. The expected principal product was chloropicrin, because chloramines are commonly assumed to react similarly to, although more slowly than, free chlorine. Different molar yields of chloropicrin were observed under acidic, neutral, and basic conditions, and surprisingly, transformation products other than chloropicrin were found. Monochloronitromethane and dichloronitromethane were detected at basic pH, and the mass balance was initially poor at neutral pH. Much of the missing mass was later attributed to nitrate formation, from a newly identified pathway involving monochloramine reacting as a nucleophile rather than a halogenating agent, through a presumed S_N2 mechanism. The study indicates that nitromethane chloramination, unlike chlorination, is likely to produce a range of products, whose speciation is a function of pH and reaction time.

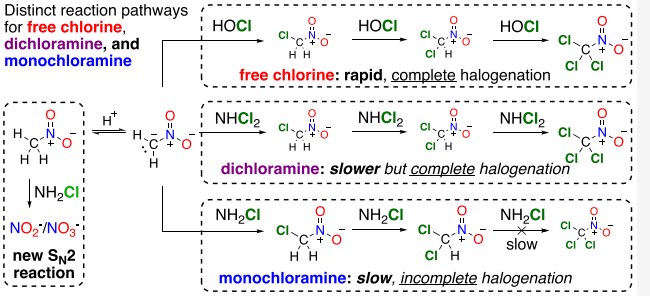

KEYWORDS: *wastewater reuse, halonitromethanes, chloropicrin, disinfection byproducts, chloramination, nitrate*

INTRODUCTION

Halonitromethanes are genotoxic nitrogenous disinfection byproducts under regulatory scrutiny,[1−4] which sometimes dominate estimates of disinfection byproduct mixture toxicity.[5,6] Formation of halonitromethanes has long been associated with the sequence of ozonation followed by chlorination.[7−10] More recently, it was shown that ozone oxidizes primary and secondary amines in natural waters and wastewater to nitro compounds, which then react with chlorine to form chloropicrin, the most frequently detected halonitromethane.[11] In our previous work, we demonstrated that ozonation of secondary wastewater effluent forms nitromethane, which is the key and possibly sole intermediate toward chloropicrin during subsequent chlorination, as might occur in direct potable reuse scenarios.[12] We further found that nitromethane formed by ozonation at the inlet of reuse plants persists through the most common advanced treatment processes used in reuse operations, such as reserve osmosis and ultraviolet light advanced oxidation processes.[13] Nitromethane remained in the final effluent water at many plants, although treatment trains employing biofiltration after ozone generally removed nitromethane well.[13] Because ozone does not leave a disinfectant residual, to meet drinking water regulations, a secondary disinfectant must to be added prior to distribution.[14] Therefore, while nitromethane in reuse effluent may not pose problems at indirect potable reuse plants where product water is discharged to an environmental barrier, in direct potable reuse operations, secondary disinfection of nitromethane-containing water is likely.

The most widely used secondary disinfectant is free chlorine (HOCl and OCl^-; i.e., bleach), but free chlorine is strongly associated with formation of many halogenated disinfection byproducts.[3,15,16] As an alternative to free chlorine, chloramines [i.e., primarily monochloramine (NH_2Cl) and trace concentrations of dichloramine ($NHCl_2$) and other species] have increased in popularity in the United States[17] because chloramines can suppress the formation of regulated trihalomethanes and haloacetic acids relative to free chlorine[15] and generally produce longer-lasting chlorine residuals than free chlorine.[17−19] Furthermore, chloramination is commonly used for disinfection and fouling control at water reuse plants,

Special Issue: Oxidative Water Treatment: The Track Ahead

Received: December 29, 2022
Revised: April 24, 2023
Accepted: May 1, 2023

Scheme 1. Reaction Pathway of Nitromethane Chlorination by Free Chlorine

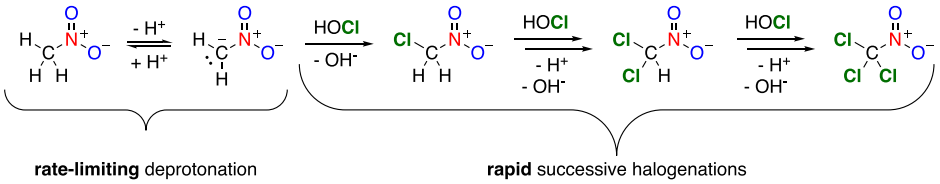

because (1) free chlorine damages the polyamide membranes most commonly used in reverse osmosis[20−22] and (2) unless very well-nitrified, most wastewater effluent contains ammonia at concentrations above what could be removed by breakpoint chlorination at practical chlorine doses, so adding free chlorine results in *in situ* chloramination.[23,24]

Inorganic chloramines are weaker oxidants than free chlorine and generally react with nucleophiles more slowly.[25,26] While the chloramination kinetics of nitromethane have not been investigated, the kinetics of chlorination of nitromethane by free chlorine have been documented. The rate-determining step (below pH ∼12) is base-catalyzed nitromethane deprotonation to form a carbanion, because deprotonation of nitromethane is slower than nitromethyl anion halogenation (Figure S1).[27] At high free chlorine concentrations, hypochlorite catalyzes the deprotonation of nitromethane (pK_a = 10.2)[28] to the corresponding nitromethyl anion ($k_{NO_2CH_3,OCl^-}$ = 2.6 × 10^{-2} M^{-1} s^{-1}),[27] and the nitromethyl anion is then oxidized by hypochlorous acid to form monochloronitromethane ($k_{NO_2CH_2^-,HOCl}$ = 9500 M^{-1} s^{-1})[27] (eqs 1−3 and Scheme 1). Chlorine substitution decreases the pK_a of the remaining methyl protons, and monochloronitromethane was assumed to be quickly chlorinated to dichloronitromethane and finally chloropicrin in a rapid cascade.[27] Enabled by this assumption, a previous study used a stopwatch to time the precipitation of chloropicrin from water after reaction initiation and, on the basis of this reaction time until precipitation and the solubility of chloropicrin, computed the reaction rate. At pH values above 11.5−12, halogenation of the nitromethyl anion by hypochlorous acid (eq 2) took over as the rate-limiting step, as nitromethane was mostly deprotonated above its pK_a of 10.2, and the reaction rate decreased at higher pH values as the proportion of free chlorine present as HOCl decreased.[27]

$$NO_2CH_3 + OCl^- \xrightarrow{slow} NO_2CH_2^- + HOCl \quad (1)$$

$$NO_2CH_2^- + HOCl \xrightarrow{fast} NO_2CH_2Cl + OH^- \quad (2)$$

$$\frac{d[NO_2CH_3]}{dt} = k_{NO_2CH_3,OCl^-}[NO_2CH_3][OCl^-] \quad (3)$$

We initially assumed that an analogous mechanism of rate-limiting deprotonation (below pH ∼12) followed by rapid halogenation might describe the chlorination of nitromethane to chloropicrin by chloramines. However, in our previous study on the fate of nitromethane in potable reuse plants employing ozone as an initial disinfectant, conversion of nitromethane to chloropicrin during subsequent chlorination of ammonia-containing wastewater (i.e., chloramination) was lower than expected. The concentrations of chloropicrin in samples collected from potable reuse plants after chlorination were lower than the concentrations of nitromethane in their prechlorination counterparts, and the samples also had detectable concentrations of monochloronitromethane and dichloronitromethane.[13] Detection of incompletely halogenated nitromethanes was surprising, because previous work indicated that mono- and dichloronitromethane were fleeting intermediates en route to chloropicrin in the presence of excess chlorine.[27] Accumulation of these intermediate species is potentially troubling, because they have been found to be more genotoxic than chloropicrin.[1] In each of the sampled water reuse plants, background ammonia in non-nitrified wastewater effluent likely led to *in situ* chloramination when free chlorine was added (i.e., chlorination of ammonia to form monochloramine and dichloramine). While substitution reactions by chlorine and chloramines often lead to similar chlorinated products (e.g., addition of chlorine to the aromatic ring of phenolic compounds),[29−32] in this case it appears that the shift from free chlorine to chloramines may have led to different products.

Our previous results on the fate of nitromethane in potable reuse plants employing chloramines and several other considerations led us to question this assumption and revisit the mechanism, beginning with the deprotonation step. (1) Past work on nitromethane chlorination used exceptionally high free chlorine concentrations (∼200 mM). At more representative concentrations, the base responsible for nitromethane deprotonation might shift to hydroxide, water, or the buffer, particularly as the second-order rate constant reported for deprotonation by hypochlorite was ∼4 orders of magnitude slower than that previously assumed for hydroxide (22 M^{-1} s^{-1}),[27] which was likely obtained by averaging two previously reported rate constants of 17.1 and 26.7 M^{-1} s^{-1}.[33] (2) Previously reported nitromethane deprotonation rate constants vary widely and were generally collected with nonselective analytical techniques available in the mid-20th century such as conductivity measurement (Table S1). (3) Chloramines are generally slower halogenating agents than free chlorine, and depending on how much slower, the crossover point for the rate-limiting step between deprotonation and halogenation might shift downward from pH 11.5−12 to a pH relevant to water treatment. (4) The previous study's assumption that subsequent halogenations of monochloronitromethane to dichloronitromethane and finally chloropicrin are so fast as to be practically instantaneous may not be valid for chloramines. Increasing the level of methyl chlorination will decrease the pK_a of the methyl proton, accelerating the reaction if deprotonation is the rate-limiting step. However, increasing the level of halogen substitution should also decrease the electron density of the conjugate base carbanion, presumably making it a less attractive target for halogenating oxidants. If halogenation rather than deprotonation were the rate-limiting step, successive halogenations might proceed in a decelerating rather than accelerating manner, potentially leading to accumulation of mono- and dihalogenated intermediates.

https://doi.org/10.1021/acs.est.2c09821
Environ. Sci. Technol. XXXX, XXX, XXX−XXX

The objectives of this study were (1) to determine the reaction mechanism of nitromethane chlorination by chloramines, (2) to determine whether monochloramine and dichloramine both react similarly with nitromethane as halogenating agents or through distinct pathways, and (3) to quantify rate constants for each elementary reaction step and develop a model for predicting rates of transformation of nitromethane by chloramines under a range of conditions.

MATERIALS AND METHODS

Materials and Reagents. Analytical standards of nitromethane (>99%) and d_3-nitromethane (99 atom % D) were purchased at the highest available purity from Sigma-Aldrich (St. Louis, MO). Standards for chloronitromethane and dichloronitromethane were purchased from CanSyn Chemical Corp. (Toronto, ON) at 99.9% purity. An analytical standard for chloropicrin (1000 μg/mL in methanol, 99.9%) was purchased from Fisher Scientific. Sodium hypochlorite solutions (4−6%), ammonium chloride (ACS reagent, ≥99.5%), and 1,2-dibromopropane (97%) were purchased from Sigma-Aldrich.

Monochloramine stocks were freshly prepared daily by slowly titrating an equal volume of a 40 mM free chlorine solution [standardized spectrophotometrically ($\varepsilon_{HOCl,292}$ = 365 M^{-1} cm^{-1})[34]] into a 48 mM ammonium chloride solution at pH 8.5−9.0. Chloramine concentrations were standardized by ultraviolet (UV) spectroscopy ($\varepsilon_{NH_2Cl,245}$ = 445 M^{-1} cm^{-1}, and $\varepsilon_{NH_2Cl,295}$ = 14 M^{-1} cm^{-1}; $\varepsilon_{NHCl_2,245}$ = 208 M^{-1} cm^{-1}, and $\varepsilon_{NHCl_2,295}$ = 267 M^{-1} cm^{-1}) as described previously,[35] immediately before use.

Chloramination Experiments. To assess the yields of product formation from nitromethane chloramination, monochloramine (0.5 mM), nitromethane (2500 μg/L = 41 μM), 1,2-dibromopropane (as an internal standard, as previously used for extraction and GC/MS measurement of halogenated DBPs[36−40] at 250 μg/L), and a buffer (10 mM) were added to triplicate 25 mL amber glass vials. A relatively high initial nitromethane concentration compared to past observations at water reuse plants[13] was chosen to permit product quantification down to potentially low molar yields with available analytical tools. Buffers that had pK_a values within 1 pH unit of the target pH were selected: acetate (pK_a = 4.76) for pH 5, phosphate (pK_{a2} = 7.21, and pK_{a3} = 12.32) for pH 7, 8, and 12, borate (pK_a = 9.2) for pH 9, and bicarbonate (pK_{a2} = 10.3) for pH 10. Reactions were conducted at a wide range of pH values because chloramines and nitromethane are both in pH-dependent equilibria; a lower bound of 5 was selected to promote increased dichloramine concentrations, and an upper bound of 12 was selected to approximately fully deprotonate nitromethane to directly observe reactions with the nitromethyl anion.

To determine approximate final reaction yields, sodium thiosulfate was added at a 1:1 molar ratio to the initial chloramine concentration to quench excess chloramines, as previously described,[41−43] after reaction for 67 h, which is in the typical range of residence times in chloraminated distribution systems (~8−100 h).[44−46] Five milliliters of the sample was withdrawn, acidified to pH 1 with a HCl solution [to ensure that mono- and dichloronitromethane (with estimated pK_a values of 7.1 and 5.9, respectively, as described below) remained protonated], and then mixed with 5 mL of methyl *tert*-butyl ether (MtBE) for liquid−liquid extraction. After the sample had been shaken for 1 min, 1 mL of the organic layer was transferred to a GC vial and injected into a GC/MS/MS instrument (Agilent 7890/7010) to quantify nitromethane, monochloronitromethane, dichloronitromethane, and chloropicrin as described previously.[12] Liquid−liquid extraction was used rather than headspace sampling to avoid potential hydrolysis of mono- and dichloronitromethane during heating of aqueous samples in the headspace sampler. In all cases, internal standard-corrected peak areas from extracted samples were compared against standard curves prepared in the same matrix as the sample (i.e., same pH and buffer concentration), spiked with the same internal standard concentration, and extracted in the same manner as experimental samples. Nitrate was measured for selected experiments (indicated in figure captions) by using the Hach Nitrate TNTplus Vial test (0.23−13.5 mg/L NO_3^-/N). Detection limits for GC/MS and IC analytes are listed in Table S2. Calibration ranges were prepared from concentrations of 0 μg/L (blank) to above the highest concentration expected to be observed for each analyte (e.g., 3000 μg/L for an initial nitromethane concentration of 2500 μg/L). All reported concentrations fell within the calibration ranges or are reported as being below the detection limit. Due to the formation of background nitrate by breakpoint chlorination,[47] controls with only monochloramine and buffer were prepared in parallel with the reaction mixture (Tables S3 and S4). The nitrate concentration at each time point was estimated by subtracting the background nitrate measured from the chloramine-only control.

To estimate the reaction rate constants, nitromethane decay was monitored during chloramination under pseudo-first-order conditions. As the buffer-catalyzed disproportionation reaction produces dichloramine from monochloramine,[48] a 1 mM monochloramine stock was prepared and left to reach equilibrium in 10 mM buffer at three different pH values (7, 9, and 11) for 24 h. Nitromethane (C_0 = 50 μM) was added to triplicate vials to initiate the reaction before the solution was transferred to glass syringes to avoid headspace formation during sampling. At each time point, an 8 mL sample was withdrawn, quenched, and acidified. A 5 mL aliquot was used to quantify nitromethane by using GC/MS/MS with headspace sampling (Agilent 7697A), and the remaining volume was injected into an ion chromatograph (Dionex Aquion) to quantify nitrate and nitrite (Figure S2). Concentrations of all analytes in each experiment were reported as the average and standard deviation of three experimental replicates.

Chloramine Speciation Modeling. To determine conditions under which the concentration of relevant chlorine species (dichloramine at pH 5 and monochloramine at higher pHs) would remain within 5% of their initial values to satisfy pseudo-first-order conditions, chloramine speciation was modeled at a range of pH values and reagent concentrations (Figure S3). Concentrations of chlorine species, including monochloramine and dichloramine, were modeled with Kintecus[49] using reaction rate constants obtained from the literature[50,51] (Table S5). This kinetic model was validated in prior publications by reproducing published chloramine speciation data[51] and by comparing model outputs to experimental data obtained during chloramination of dimethylamine.[52] These concentrations were later used for rate constant determination as described below.

Deprotonation Rate Experiments. Nitromethane is a weak acid (pK_a = 10.2), and its deprotonation has previously

https://doi.org/10.1021/acs.est.2c09821
Environ. Sci. Technol. XXXX, XXX, XXX−XXX

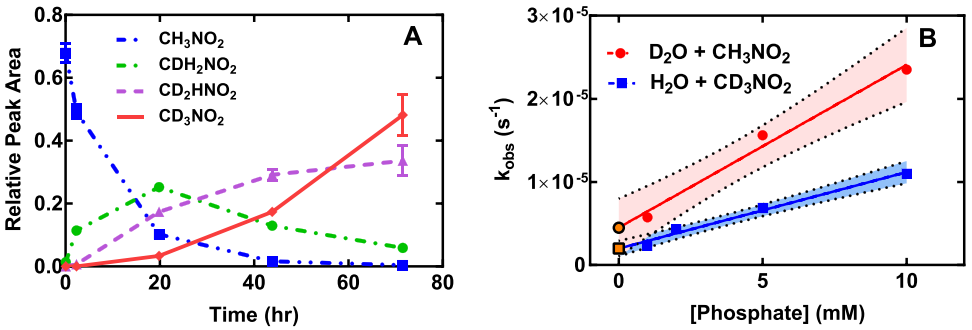

Figure 1. (A) Relative peak areas (normalized to the internal standard peak area) of nitromethane and deuterated nitromethanes with respect to time. Experimental details: $[\text{nitromethane}]_0$ = 16.4 μM (1000 μg/L), [1,2-dibromopropane] = 4.9 μM (1000 μg/L) (internal standard), D_2O as the solvent, $[PO_4]_{TOT}$ = 10 mM, pH 8. Error bars represent the range of experimental triplicates. (B) Linear regression of observed rate constants measured in water and heavy water with respect to phosphate buffer concentrations. Orange symbols represent *y*-intercepts extrapolated from linear regression. Shaded areas around regression lines represent the 95% confidence interval around the regression. Regression error terms are provided in Table S7.

been reported to be rate-limiting at neutral to modestly alkaline pH during chlorination of nitromethane.[27] Measuring the rate of acid deprotonation is not as straightforward as measuring its pK_a, because the conjugate base product of the reaction can become protonated and return to the acidic form. Therefore, approaches to measuring deprotonation rates typically rely on capturing the conjugate base to form a different, measurable product.[53] In this study, nitromethane deprotonation rate constants were measured by observing the conversion of light nitromethane (CH_3NO_2) to heavy nitromethane (CD_3NO_2) in D_2O (Scheme S1) and conversely the conversion of deuterated nitromethane to light nitromethane in water with mass spectrometry. Because the maximum contribution of ordinary protons to D_2O solution at the dilute nitromethane concentration evaluated is negligible, the back reaction (e.g, replacement of a deuteron from CH_2DNO_3 with a proton from trace HDO or H_2O) was neglected.

Because deprotonation reactions can be base-catalyzed, multiple buffer concentrations were used, allowing the generation of a buffer dilution plot to estimate the non-buffer-catalyzed (i.e., specific base-catalyzed) reaction rate constant. To account for potential kinetic isotope effects in the deprotonation rate, experiments under identical conditions except with d_3-nitromethane in ordinary water were also performed and analyzed similarly.

Reaction mixtures for deprotonation rate experiments were prepared in triplicate 250 mL glass beakers. The initial concentration of nitromethane was 1 mg/L, and 1,2-dibromopropane (250 μg/L) was used as the internal standard to control for extraction efficiency. The total ionic strength of the solution was fixed at 20 mM with supplemental sodium chloride, accounting for the ionic strength contribution from each buffer concentration. At each time point, 5 mL of the sample was withdrawn, acidified, and immediately extracted with 5 mL of MtBE. After the sample had been shaken for 1 min, the organic layer was transferred into a 15 mL centrifuge tube and dewatered with magnesium sulfate (to avoid further proton exchange). After dewatering, samples were injected into the GC/MS instrument, with the same method as described previously for nitromethane,[12] except for the addition of additional mass transitions to account for heavy isotopes of nitromethane. Four different mass transitions were monitored: m/z 64 to 46, m/z 63 to 46, m/z 62 to 46, and m/z 61 to 46 for tri-, di-, mono-, and unlabeled nitromethane, respectively. In each case, the fragment ion had the same mass because the fragmentation step removed the methyl group and the resulting fragment was the nitro group, the mass of which was unaffected by mass labeling or deuterium exchange.

Rate Constant Estimation. To estimate nitromethane reaction rate constants with chloramines, overall reaction rate laws were constructed for reactions leading to changes in concentrations of nitromethane (Text S1, eq S5), nitromethyl anion (eq S6), and total nitromethane (eq S7). These differential equations, along with modeled chloramine concentrations (Table S6) and experimental nitromethane, nitrite, and nitrate data (Figure S4), were used to numerically fit rate constants using the GEKKO optimization suite for Python 3,[54] by minimizing the sum of squared errors between measured and predicted concentrations. Further details are available in Text S2. A numerical approach for obtaining rate constants was employed rather than the more conventional pseudo-first-order approach, because the latter would require that nitromethane maintain acid−base equilibrium with its conjugate base anion (i.e., that deprotonation is not rate-limiting), which was shown not to be true previously during nitromethane chlorination.[27]

RESULTS AND DISCUSSION

Nitromethane Deprotonation Rate. Acid−base reactions in environmental contexts are typically assumed to be at equilibrium. However, in certain cases, when the acid or base species is consumed by a subsequent reaction, the proton transfer reaction between acid and base species may be rate-limiting, as hypothesized recently for the ozonation of carbanions.[55] Therefore, we sought to measure the deprotonation reaction rate constant of nitromethane in water, so that this reaction step could be included in overall kinetic considerations of nitromethane chloramination.

When light nitromethane was added to D_2O, the concentration of light nitromethane decreased over time (Figure 1A), and successively more deuterium-labeled nitromethane was formed (i.e., first CDH_2NO_2, then CD_2HNO_2, and then CD_3NO_2). To account for general base catalysis, a series of these experiments were conducted at a range of phosphate buffer concentrations. The observed first-order rate constants for loss of nitromethane or deuterated nitromethane in D_2O or H_2O, respectively, were plotted versus buffer concentration, allowing both estimation of the buffer-catalyzed

https://doi.org/10.1021/acs.est.2c09821
Environ. Sci. Technol. XXXX, XXX, XXX−XXX

rate constant and extrapolation to estimate the unbuffered rate constant (Figure 1B). At pH 8, the extrapolated observed rate constant of deprotonation in heavy water with no buffer was estimated to be $(4.5 \pm 0.8) \times 10^{-6}$ s^{-1}, corresponding to a second-order deprotonation rate constant (k_{OD^-}) (before correcting for isotope effects) of 4.5 ± 0.8 M^{-1} s^{-1}.

When the reaction is observed in D_2O, a solvent kinetic isotope effect is expected.[56−58] To make a second estimate of the deprotonation rate constant, while avoiding this solvent kinetic isotope effect from D_2O, similar experiments were carried out in a reverse fashion by dissolving deuterium-labeled nitromethane in water (Figure S5). The observed rate constants in H_2O at the same buffer concentrations as those measured in D_2O were noticeably slower, as was the estimated non-buffer-catalyzed rate constant [$(1.98 \pm 0.29) \times 10^{-6}$ s^{-1}, corresponding to a k_{OH^-} of 1.98 ± 0.29 M^{-1} s^{-1}] (Figure 1B and Table S7). However, with deuterium-labeled nitromethane, a primary kinetic isotope effect is expected (i.e., slower reaction for a deuterated vs protonated compound when the deuterium or hydrogen is involved in the rate-limiting step), as the heavier deuterium depresses the vibrational zero-point bond energy compared to hydrogen.[57]

Neither scenario can eliminate the interference of deuterium, but previous estimates of primary, secondary, and solvent isotope kinetic effects allow correction of both values to estimate the true rate constant for deprotonation of nitromethane by hydroxide. The solvent kinetic isotopic effect reported for deprotonation of several nitroalkanes in heavy water was averaged to be 1.4,[59] and after correction for the difference between the pH measured with a probe and pD,[60] and the difference in K_w between D_2O and H_2O, the true rate constant for nitromethane deprotonation from our experiment in D_2O was estimated to be 11.6 ± 2.1 M^{-1} s^{-1} (Text S3).

The primary kinetic isotope effect of the nitromethane proton versus deuteron exchange with hydroxide was previously found to be 10.3,[61] but this estimate neglected α-secondary isotope effects arising from additional deuteriums bonded to the same carbon as the departing deuteron. The secondary kinetic isotope effect for dedeuteration of a multiply deuterated carbon was estimated as 1.15 per extra deuterium, leading to a value of $1.15^2 = 1.32$ for fully deuterated methyl carbons,[59] and a secondary-corrected primary kinetic isotope effect for nitromethane deprotonation of $k_H/k_D = 10.3/1.32 = 7.8$. Applying these corrections to data acquired from our experiments with deuterated nitromethane in water, we estimated the true rate constant for nitromethane deprotonation in water to be 15.4 ± 2.3 M^{-1} s^{-1} (Text S3), which agrees within 25% with the results of the experiments performed in a reverse fashion. For subsequent calculations, we averaged the results from both approaches for a final value of 13.5 ± 1.6 M^{-1} s^{-1}.

Chloramination of Nitromethane. The yields of monochloronitromethane, dichloronitromethane, and chloropicrin during chloramination of nitromethane were measured at a range of pH values (Figure 2). At all pH values, nitromethane remained detectable after reaction with chloramines for 67 h, indicating that reactions of nitromethane with chloramines are much slower than that with free chlorine, which had half-lives on the order of minutes over a similar range of pH values.[27] More nitromethane remained after chloramination at neutral pH than at higher pH, suggesting that the overall rate of nitromethane chloramination increases with pH within this range. This is consistent with chlorination

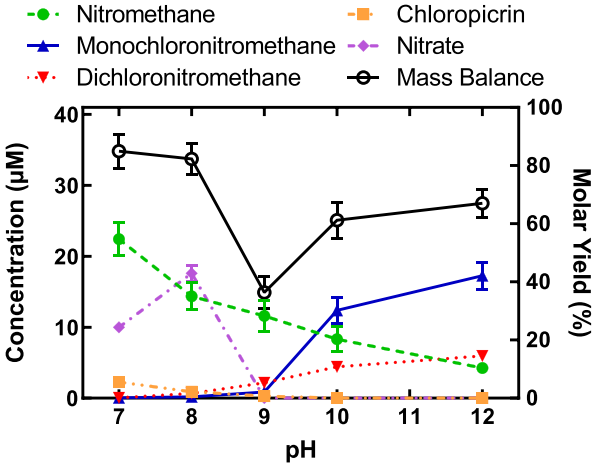

Figure 2. Products of nitromethane chloramination as a function of pH, and nitrogen mass balance (right *y*-axis) calculated as the sum of the concentration of all five compounds (nitromethane, halonitromethanes, and nitrate). Analytes were quantified by the Hach TNT kit (nitrate) and GC/MS/MS (all other analytes). Experimental details: reaction time of 67 h, $[\text{nitromethane}]_0 = 41$ μM (2500 μg/L), and $[\text{monochloramine}]_0 = 10$ mM. For pH 7, 8, and 12, $[PO_4]_{TOT} = 10$ mM. For pH 9, [borate] = 10 mM. For pH 10, $[CO_3^{2-}] = 10$ mM. Error bars represent the standard deviation of experimental triplicates. Error bars for the mass balance are standard deviations statistically propagated from the standard deviations of summed concentrations. Nitrate concentrations were below the detection limit at pH 9−12.

of nitromethane; the rate-limiting step of nitromethane chlorination by free chlorine below pH 11.5−12 is deprotonation of nitromethane, which is significantly faster at higher pH.[27]

By accounting for only nitromethane, monochloronitromethane, dichloronitromethane, and chloropicrin, we found nitrogen mass balances were poor (36−60%), especially at pH 7−9. At higher pH, mass balance recovered. This indicated that at neutral pH, other products besides chlorinated nitromethanes were formed, which was not observed for chlorination of nitromethane with free chlorine.[27] By measuring nitrate in the same samples, an ∼90% mass balance was achieved at pH 7 and 8. Nitrate formation peaked at pH 8, and the suspected reaction leading to nitrate formation, a substitution reaction first producing nitrite that is subsequently oxidized to nitrate, is discussed below. While nitrite was not measured in this experiment, in a subsequent experiment discussed below, nitrite formation peaked at approximately 35% molar yield at pH 9, potentially explaining the missing mass balance, even after including nitrate, in Figure 2.

The molar yield of chloropicrin was unexpectedly low and decreased with an increase in pH. Meanwhile, the yields of monochloronitromethane and dichloronitromethane increased significantly under basic conditions, and the total halonitromethane yield increased at higher pH. The production of more monochloronitromethane and dichloronitromethane than chloropicrin is contrasted by reactions with free chlorine, in which the initial chlorine addition was always assumed to be the rate-limiting step toward chloropicrin, and the secondary and tertiary chlorine additions were nearly instantaneous.[27] The pK_a values of monochloronitromethane and dichloronitromethane were estimated through pH titration with potassium hydroxide and were 7.1 and 5.9, respectively (Figure S6). The

https://doi.org/10.1021/acs.est.2c09821
Environ. Sci. Technol. XXXX, XXX, XXX−XXX

results of our pH titrations of incompletely chlorinated nitromethane species indicate that at or above neutral pH, dichloronitromethane (pK_a < 7) should be predominantly present as an environmentally stable carbanion, the first such example of which we are aware among aquatic contaminants. A decreased pK_a with an increased level of chlorine substitution was expected, due to the inductive effect of electron-withdrawing groups on acidity. At mildly alkaline pH, for both monochloronitromethane and dichloronitromethane, the predominant species would therefore be the deprotonated conjugate base, which is suspected to be the direct target of halogenation reactions. In addition to depressing pK_a, increasing the level of chlorine substitution is expected to decrease the electron density of the carbanion, likely decreasing the rates of subsequent chlorine addition. Consequently, even though at alkaline pH a higher proportion of chlorinated nitromethyl anions are available for halogenation relative to nitromethane, a lower concentration of chloropicrin was detected than monochloronitromethane and dichloronitromethane, likely due to slower anion chlorination with an increasing level of chlorine substitution. Thus, monochloronitromethane and dichloronitromethane are expected to be the final reaction products of chloramination at highly alkaline pH values (10−12), and the concentration of partially chlorinated halonitromethanes exceeded that of chloropicrin at pH 9. This is consistent with our prior observation of mono- and dichloronitromethane concentrations sometimes in excess of chloropicrin concentrations in ozonated wastewater from pilot- and full-scale reuse systems that had subsequently been chloraminated.[13]

Next, we evaluated the formation of these species from chloramines over time, and in parallel, the concentration of chloramine species was modeled, to enable computation of pseudo-first-order rate constants. At pH 5.1, ammonia chlorination initially produced monochloramine, which was rapidly converted to dichloramine, and dichloramine remained at approximately steady state for the duration of the experiment after the first several minutes. At pH 8.3 and 9.9, monochloramine dominated and the formation of dichloramine was minimal (Figure S3).

At acidic pH (5.1), near the value typically observed in the reverse osmosis permeate of water reuse operations,[51] the reaction was very slow as expected, because the rate of deprotonation of nitromethane should be low; therefore, the reaction was monitored over a longer time scale than at more alkaline pH (Figure 3A). Nitrate formation was negligible. The predominant chlorinated product was chloropicrin, and the rate of chloropicrin formation increased (Figure 3A) after monochloramine was converted to dichloramine (Figure S3), consistent with preferential halogenation of nitromethane by dichloramine over monochloramine. Dichloramine has been previously reported to halogenate another nucleophile, triclosan, >3 orders of magnitude faster than monochloramine,[31] suggesting that it is a more potent halogenating agent than monochloramine. The mass balance remained relatively constant over the course of the reaction, likely due to the small fraction of nitromethane depleted. Overall, complete halogenation to chloropicrin was the primary fate of consumed nitromethane under acidic chloramination conditions.

At a slightly alkaline pH (8.3) typical of final product water at reuse plants,[51] nitromethane reacted much faster with chloramines (Figure 3B). The concentrations of monochloronitromethane and dichloronitromethane first increased and

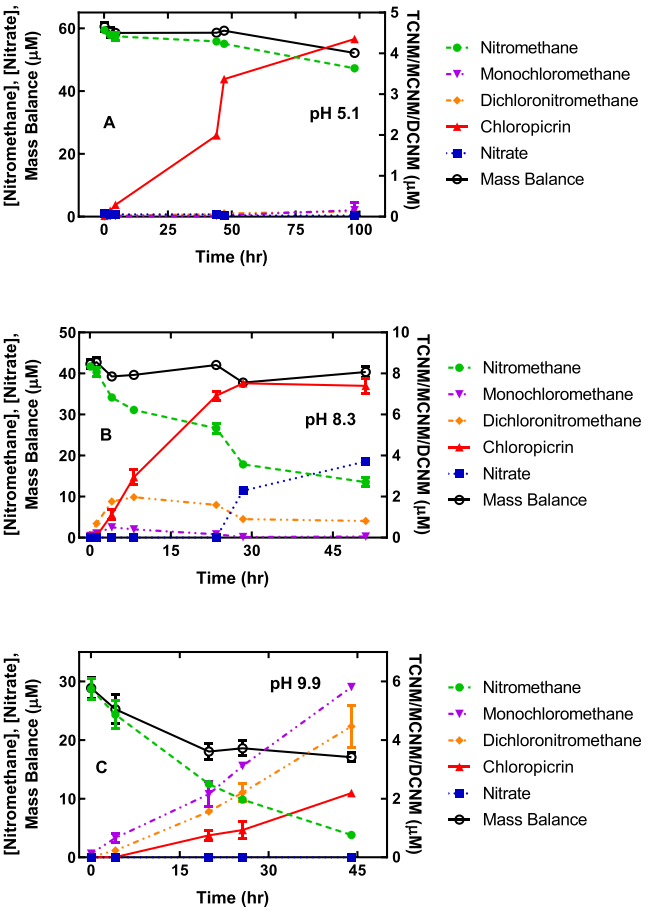

Figure 3. Chloramination of nitromethane to its corresponding chlorinated products and nitrate at nominal pH values of 5, 8, and 10. Left *y*-axis: nitrate (measured by the Hach TNT kit) and nitromethane concentrations, and nitrogen mass balance. Right *y*-axis: chloropicrin (TCNM), dichloronitromethane (DCNM), and monochloronitromethane (MCNM) concentrations. Experimental details: nominal $[\text{nitromethane}]_0$ = 2500 μg/L (41 μM). For pH 5.1, $[HOCl]_0$ = 2.5 mM, $[NH_4Cl]_0$ = 2 mM, and $[\text{acetate}]_{TOT}$ = 10 mM. For pH 8.3, $[HOCl]_0$ = 1.5 mM, $[NH_4Cl]_0$ = 2 mM, and $[PO_4]_{TOT}$ = 2.5 mM. For pH 9.9, $[HOCl]_0$ = 1.5 mM, $[NH_4Cl]_0$ = 2 mM, and $[CO_3]_{TOT}$ = 2.5 mM. Error bars represent the standard deviation of experimental triplicates. Error bars for mass balance are standard deviations statistically propagated from the standard deviations of summed concentrations. Nitrate concentrations were below the detection limit in panels A and C and before 24 h in panel B.

then decreased. The concentration of chloropicrin, as the final product of halogenation, increased and plateaued at a molar yield of 17% relative to the initial nitromethane concentration. Although chloropicrin was the dominant final halogenated product, incompletely halogenated species dominated during the first few hours, which is potentially relevant to a possible direct potable reuse scenario in which recycled water is conveyed directly to a water treatment plant. Nitrate was the most abundant product from the reaction, with a 41% molar yield. Mass balance remained approximately constant and complete (~80−90%) throughout the process, indicating that nitrate formation and successive halogenation of nitromethane are the dominant reactions.

At more alkaline pH (9.9), potentially relevant to water after lime softening, a low level of nitrate formation was observed (Figure 3C), and chlorinated nitromethanes were the major

https://doi.org/10.1021/acs.est.2c09821
Environ. Sci. Technol. XXXX, XXX, XXX−XXX

Scheme 2. Proposed Pathways of Reactions of Nitromethane with Chloramines[a]

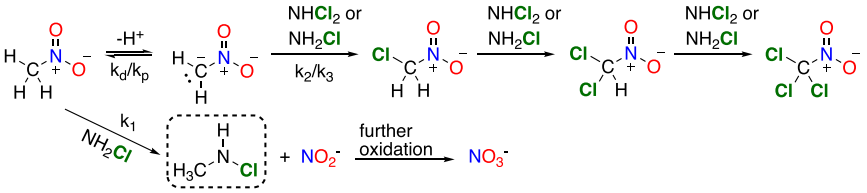

[a]The product depicted in the dashed box was presumed but not directly observed.

products. Monochloronitromethane was formed quickly, and the concentration increased with respect to time. Substantial concentrations of dichloronitromethane were also formed, while a lower level of chloropicrin was detected compared to those at pH 5.1 and 8.3, indicating that at alkaline pH, chlorination by chloramines is likely to be incomplete under realistic time scales. The pK_a values of monochloronitromethane and dichloronitromethane were found to be 7.1 and 5.9, respectively (Figure S6). Therefore, at basic pH, these two compounds should be predominantly deprotonated, implying that the rate-limiting step for subsequent reactions should be halogenation rather than deprotonation. Substantial accumulation of monochloronitromethane and dichloronitromethane under alkaline conditions favoring monochloramine, but not acidic conditions favoring dichloramine, suggests that dichloramine is a sufficiently powerful halogenating agent to chlorinate the dichloronitromethyl anion to chloropicrin under realistic time scales while monochloramine is not. Mass balance declined over time, potentially due to the accumulation of nitrite, which was not measured in this experiment, at high pH, as discussed below.

To rule out a potential role for HOCl (in equilibrium with chloramines) in nitromethane oxidation during chloramination, we computed expected first-order rate constants for nitromethane by HOCl at each of these pH values. HOCl concentrations at 24 h (selected at roughly the midpoint of the experiment in Figure 3) were obtained from the chloramine speciation model output used to create Figure S3 and multiplied by the previously reported rate constant for HOCl oxidation of the nitromethyl anion,[27] and the proportion of nitromethane present in the anionic form (conservatively assuming acid−base equilibrium is maintained) (Text S4). These first-order rate constants were converted to half-lives and were 23.1 years at pH 5.1, 64 days at pH 8.3, and 138 h at pH 9.9. Therefore, we conclude that the contribution of HOCl to nitromethane chlorination under chloramination conditions is minimal.

Reaction Mechanism. The reaction mechanism was further investigated, in particular the unexpected nitrate formation. Because the level of nitrate formation peaked at pH 8, which is roughly halfway between the pK_a of nitromethane (10.2) and the pseudo-pK_a at which monochloramine and dichloramine are approximately equally abundant (pH 6.1) (Figure S7), we concluded that nitrate is formed from the reaction between monochloramine and neutral nitromethane.

We suspected that with the lone pair of electrons on its nitrogen, monochloramine can potentially serve as a nucleophile. Nucleophilic attack by monochloramine has been previously proposed to explain haloacetonitrile formation, by attack of the monochloramine nitrogen on carbonyl functional groups in NOM.[42,43,62,63] Because the nitro group is strongly electron withdrawing,[57] the carbon of nitromethane is relatively electron deficient and may potentially be available for reactions with nucleophiles. We therefore suspect that an S_N2 nucleophilic substitution reaction between monochloramine and nitromethane explains nitrate formation. In such a reaction, the departing nitro group would form nitrite, and subsequent nitrite oxidation by chloramines would lead to nitrate formation ($k_{NO_2^-,NH_2Cl,H^+}$ = 7.6 × 10^6 M^{-2} s^{-1}).[47] The corresponding half-life for nitrite oxidation at pH 8 would be approximately 1 h, indicating that at alkaline pH, detectable nitrite might accumulate, as further explored below. To rule out the production of nitrate from trace ammonia, which is also present in chloramine mixtures, a control experiment was performed by combining nitromethane with the amount of ammonia estimated to be present in the system during chloramination (Table S8), and no nitrate was detected (Figure S8), suggesting that nitrate formation by nucleophilic substitution reactions between nitromethane and trace ammonia is negligible under relevant time scales. However, in ammonia-containing water with no chlorine, substitution by ammonia, which we suspect is more intrinsically nucleophilic than monochloramine, might drive the production of nitrite from nitromethane, especially at alkaline pH.

Finally, to rule out significant hydrolysis of nitromethane, monochloronitromethane, dichloronitromethane, and chloropicrin to nitrate or nitrite in water, control experiments were performed in the absence of chloramines. First, nitromethane and the three halonitromethanes were placed in buffered deionized water at pH 12 (to maximize the concentration product of neutral nitromethane and hydroxide), and no reaction was observed (Figure S9). Highly alkaline conditions were chosen because little nitrate was observed at acidic pH (Figure 3A), suggesting that if hydrolysis were responsible, base-catalyzed rather than acid-catalyzed hydrolysis would likely promote nitrate formation. Next, a control experiment with the same four compounds at initial concentrations of 10 μM each was performed at pH 8 (where maximum nitrate formation was observed in Figure 2). A small amount of nitrate, possibly from trace contamination of the buffer, was detected but did not increase throughout the experiment. Nitrite concentrations did gradually increase, but to only 0.5 μM at 72 h (Figure S10A), corresponding to a maximum 5% molar yield [if only one of the four (halo)nitromethanes were hydrolyzing, less if multiple species produced nitrite], suggesting that ≤10% of the nitrate formation observed at pH 8 in Figure 2 was due to hydrolysis reactions producing nitrite and subsequent oxidation to nitrate. Because chloropicrin has been previously observed to be stable in water (<10% decay in 1 week),[64] the stabilities of monochloronitromethane and dichloronitromethane were evaluated, and no significant decay was observed (Figure S10B). A proposed overall reaction mechanism is shown as Scheme 2,

https://doi.org/10.1021/acs.est.2c09821
Environ. Sci. Technol. XXXX, XXX, XXX−XXX

incorporating successive deprotonation and halogenation reactions competing with the substitution reaction leading to nitrite and nitrate formation, with the putative (but not directly observed) side product from the monochloramine reaction with nitromethane shown in a dashed box.

Estimating Chloramination Rate Constants. To further understand the reactions of nitromethane with chloramines, a kinetic model was constructed for the depletion of nitromethane (eqs 4−8) and used for fitting rate constants to our data in Python (Text S2).

$$OH^- + CH_3NO_2 \xrightarrow{k_d} CH_2NO_2^- + H_2O \quad (4)$$

$$H_2O + CH_2NO_2^- \xrightarrow{k_p} CH_3NO_2 + OH^- \quad (5)$$

$$NH_2Cl + CH_3NO_2 \xrightarrow{k_1} NO_2^- \rightarrow NO_3^- \quad (6)$$

$$NH_2Cl + CH_2NO_2^- \xrightarrow{k_2} CH_2ClNO_2 \quad (7)$$

$$NHCl_2 + CH_2NO_2^- \xrightarrow{k_3} CH_2ClNO_2 \quad (8)$$

To account for buffer catalysis in the deprotonation rate constant (k_d), the buffer catalysis rate constant was obtained from the slope of the buffer dilution plot (Figure 1B and Table S7) constructed from nitromethane deprotonation rate constants collected in water at a range of buffer concentrations ($k_{buffer} = 9.19 \times 10^{-4}$ M^{-1} s^{-1}) and assumed to be the similar for phosphate and carbonate, as base-catalyzed buffer catalysis rates for carbon acid deprotonation by anionic buffers[65,66] appear to be less species-dependent than, e.g., those for acid-catalyzed monochloramine disproportionation reactions, especially near the pK_a of the buffer,[67] a condition we maintained throughout our experiments. The overall deprotonation rate constant used in the model was the sum of the hydroxide ($k_{OH^-} = 13.5$ M^{-1} s^{-1}) and the buffer-catalyzed rate constants (i.e., $k_d = k_{OH^-}[OH^-] + k_{buffer}[buffer]$) (Text S1), and the reprotonation rate of nitromethyl anion was treated as an unknown variable to be solved for by the model, to account for possible buffer-catalyzed reprotonation. Because the model was underconstrained without a known nitromethyl anion reprotonation rate constant, first the formation rate constant of the two inorganic nitrogen species was used to determine the rate constant (k_1) of the suspected S_N2 nucleophilic substitution reaction of nitromethane and monochloramine shown in Scheme 2. Then, the rate expressions for changes in the concentration of nitromethane and nitromethyl anion and the sum of the two species (Text S1 and eqs S5−7) were used to fit the experimental nitromethane, nitrate, nitrite, monochloramine, and dichloramine concentrations (Figure S4) in Python to estimate k_2 and k_3 as described in Text S2. These data were collected at a wide range of pH values and increased concentrations, not necessarily representative of water treatment conditions, to produce sufficiently substantial differences in reagent concentrations (monochloramine, dichloramine, nitromethane, and nitromethyl anion) to permit rate constant fitting for each reaction involved.

According to our computational estimates, the S_N2 nucleophilic substitution rate constant is the slowest ($k_1 = 3.07 \times 10^{-3}$ M^{-1} s^{-1}), and dichloramine ($k_3 = 72.0$ M^{-1} s^{-1}) is a faster halogenating agent than monochloramine ($k_2 = 1.32 \times 10^{-2}$ M^{-1} s^{-1}) by approximately 4 orders of magnitude, which is consistent with, but somewhat greater than, previous values for chloramination of two other classes of nucleophile: triclosan[31] and organophosphorous pesticides.[68] These values correspond to the pseudo-first-order rate constants ($k_1 = 1.4 \times 10^{-6}$ s^{-1}, $k_3 = 4.4 \times 10^{-3}$ s^{-1}, and $k_2 = 6.6 \times 10^{-6}$ s^{-1}) at the initial monochloramine (0.456 mM) and dichloramine (60.9 μM) concentrations estimated at pH 7 (Table S6), indicating that the greater intrinsic reactivity of dichloramine is sufficient to overcome its lower abundance than monochloramine at neutral pH, and dichloramine likely serves as the predominant oxidant in this pathway. The greater disparity in chloramine reactivities toward nitromethyl anion compared to other, faster-reacting nucleophiles is consistent with the reactivity−selectivity principle, in which slower reactions are more selective than faster reactions.[57] By using these rate constants, the concentrations of the three species were predicted and plotted against measured values to determine the quality of the model fit (Figure S11). The predicted values of nitromethane decay at pH 7 and 11 agree well with the experimental data, and at pH 9, the model predicts a slightly slower decay. For nitrate and nitrite formation, the model agrees well with experimental data at pH 9 and 11, while at pH 7, formation was slightly underpredicted. Regrettably, the algorithm used to numerically solve for rate constants does not report standard deviations of output values, so the reported rate constants should be considered estimates; nonetheless, the predicted concentrations generally agreed within ∼10% of experimental values, and always within ∼30%.

Predicted nitromethyl anion concentrations generally decreased in proportion to nitromethane concentrations (Figure S12), potentially suggesting that nitromethane remained in an acid−base equilibrium with the nitromethyl anion. However, at pH 9 and 11, nitromethyl anion concentrations were significantly lower than would be predicted by simple equilibrium calculations (e.g., 2.97 and 43.2 μM, respectively, at $t_{rxn} = 0$), consistent with rate-limiting deprotonation rather than halogenation.

The measured and modeled concentrations of inorganic nitrogen species support our hypothesis that the initial product of reactions of nitromethane with monochloramine is nitrite, which is subsequently oxidized to nitrate, as nitrite concentrations exceeded nitrate levels at pH 9 and 11 (Figure S11), which may explain the missing balance observed in Figure 3 under alkaline conditions, when nitrite was not measured. More accumulation of nitrite at alkaline pH than at neutral pH is consistent with lower concentrations of dichloramine relative to monochloramine at alkaline pH. Dichloramine is a stronger oxidant than monochloramine, and monochloramine dominates under alkaline conditions; hence, nitrite would be oxidized to nitrate more quickly at neutral pH than at alkaline pH. Less nitrite production at pH 11, where nitromethane is predominantly in the anionic form, than at pH 9 is consistent with neutral nitromethane rather than the nitromethyl anion serving as the target for substitution by monochloramine.

These results once again suggest that monochloramine is less important than dichloramine in transforming nitromethane into toxic chloronitromethanes, and instead, it can convert nitromethane into nitrite or nitrate. Even though the monochloramine nucleophilic substitution reaction rate constant ($k_1 = 3.07 \times 10^{-3}$ M^{-1} s^{-1}) is smaller than the rate constant of its nitromethyl anion halogenation reaction ($k_2 = 1.32 \times 10^{-2}$ M^{-1} s^{-1}), rate-limiting deprotonation of nitromethane decreases the availability of the nitromethyl

https://doi.org/10.1021/acs.est.2c09821
Environ. Sci. Technol. XXXX, XXX, XXX−XXX

anion relative to neutral nitromethane. The corresponding first-order rate constants, based on the estimated initial concentrations of nitromethane (40 μM) and the nitromethyl anion (0.02 μM) at pH 7 (Figure S12), would be as follows: $k_1' = 1.2 \times 10^{-7}$ s^{-1}, and $k_2' = 2.6 \times 10^{-10}$ s^{-1}. These values are consistent with faster substitution than halogenation by monochloramine near neutral pH. These results suggest that efforts to minimize dichloramine formation during wastewater chloramination to avoid nitrosamine formation[23,24,51] may also minimize formation of chlorinated nitromethanes.

Implications. Previously, we observed incomplete halogenation of nitromethane in chloraminated recycled effluent from full-scale water reuse plants, in contrast to chlorinated effluent in which successively faster chlorination reactions quantitatively convert nitromethane to chloropicrin. In this study, we found that halogenation of nitromethane by chloramines is slow enough that incompletely halogenated products, which have been reported to be more toxic than chloropicrin, may accumulate under certain conditions. At low pH values near the pH of typical reverse osmosis permeate in water reuse operations, nitromethane chloramination is slow enough that it will likely not be significantly transformed before UV/AOP treatment, through which it was previously shown to persist. At the slightly alkaline pH typical of finished recycled water, nitromethane chloramination was relatively slow ($t_{1/2} \sim$ 24h), and the predominant halogenated product was dichloronitromethane within the first few hours and remained detectable for 48 h, even as its concentration was surpassed by that of chloropicrin. Dichloronitromethane may therefore pose a risk in "flange-to-flange" direct potable reuse schemes, in which recycled wastewater is sent directly into water supplies, if the water is never exposed to free chlorine. Finally, at the high pH typical of lime softening operations, monochloronitromethane was the predominant product. Formation of monochloronitromethane at high pH highlights a potential risk for drinking water or wastewater reuse plants with ozone primary disinfection followed by lime softening, as practiced by some RO-free reuse plants,[69] depending on the final pH after recarbonation and the choice of secondary disinfectant. Beyond consideration of nitromethane chloramination reactions, this study highlights that (1) acid/base reactions of environmentally relevant nucleophiles are not always at equilibrium (i.e., deprotonation can be rate-limiting), (2) monochloramine may react with electrophiles through a previously overlooked nucleophilic substitution pathway, and (3) dichloramine may be underappreciated as a halogenating agent relative to monochloramine, despite its typically low concentrations in combined chlorine mixtures.

■ ASSOCIATED CONTENT

Supporting Information

The Supporting Information is available free of charge at https://pubs.acs.org/doi/10.1021/acs.est.2c09821.

Details of the analytical methods, rate and equilibrium constants, regression parameters, deprotonation rate calculations, modeled chloramine speciation, additional kinetic data, titration curves, example chromatograms, and kinetic modeling inputs and outputs (PDF)

■ AUTHOR INFORMATION

Corresponding Author

Daniel L. McCurry − *Astani Department of Civil and Environmental Engineering, University of Southern California, Los Angeles, California 90089, United States;* orcid.org/0000-0002-5599-2540; Phone: (213) 740-0762; Email: dmccurry@usc.edu

Authors

Jiaming Lily Shi − *Astani Department of Civil and Environmental Engineering, University of Southern California, Los Angeles, California 90089, United States;* Present Address: Department of Civil and Environmental Engineering, Stanford University, Stanford, CA 94305

Euna Kim − *Astani Department of Civil and Environmental Engineering, University of Southern California, Los Angeles, California 90089, United States*

Georgia B. Cardosa − *Astani Department of Civil and Environmental Engineering, University of Southern California, Los Angeles, California 90089, United States;* Present Address: Department of Civil and Environmental Engineering, University of California, Berkeley, Berkeley, CA 94720.

Complete contact information is available at: https://pubs.acs.org/10.1021/acs.est.2c09821

Author Contributions

[§]J.L.S. and E.K. contributed equally to this work.

Notes

The authors declare no competing financial interest.

■ ACKNOWLEDGMENTS

J.L.S. was partially supported by a T. F. Yen Fellowship. G.B.C. was supported by a University of Southern California (USC) Provost's Undergraduate Research Fellowship. The authors acknowledge additional funding from the National Science Foundation (Grants CBET-1944810 and CHE-2003472). The authors thank Profs. Kristopher McNeill (ETH-Zürich, Zürich, Switzerland), Valery Fokin (USC), and John Sivey (Towson University, Towson, MD) for helpful discussions and Marco Kleimans (USC) for experimental assistance.

■ REFERENCES

(1) Plewa, M. J.; Wagner, E. D.; Jazwierska, P.; Richardson, S. D.; Chen, P. H.; McKague, A. B. Halonitromethane drinking water disinfection byproducts: chemical characterization and mammalian cell cytotoxicity and genotoxicity. *Environ. Sci. Technol.* **2004**, *38* (1), 62−68.

(2) Plewa, M. J.; Kargalioglu, Y.; Vankerk, D.; Minear, R. A.; Wagner, E. D. Mammalian cell cytotoxicity and genotoxicity analysis of drinking water disinfection by-products. *Environ. Mol. Mutagen.* **2002**, *40* (2), 134−42.

(3) Krasner, S. W.; Weinberg, H. S.; Richardson, S. D.; Pastor, S. J.; Chinn, R.; Sclimenti, M. J.; Onstad, G. D.; Thruston, A. D. Occurrence of a new generation of disinfection byproducts. *Environ. Sci. Technol.* **2006**, *40* (23), 7175−7185.

(4) Stalter, D.; O'Malley, E.; von Gunten, U.; Escher, B. I. Mixture effects of drinking water disinfection by-products: implications for risk assessment. *Environ. Sci.: Water Res. Technol.* **2020**, *6* (9), 2341−2351.

(5) Cuthbertson, A. A.; Kimura, S. Y.; Liberatore, H. K.; Summers, R. S.; Knappe, D. R.; Stanford, B. D.; Maness, J. C.; Mulhern, R. E.; Selbes, M.; Richardson, S. D. Does granular activated carbon with chlorination produce safer drinking water? From disinfection

byproducts and total organic halogen to calculated toxicity. *Environ. Sci. Technol.* **2019**, *53* (10), 5987−5999.
(6) McKenna, E.; Thompson, K. A.; Taylor-Edmonds, L.; McCurry, D. L.; Hanigan, D. Summation of disinfection by-product CHO cell relative toxicity indices: sampling bias, uncertainty, and a path forward. *Environ. Sci.: Processes Impacts* **2020**, *22* (3), 708−718.
(7) Thibaud, H.; De Laat, J.; Merlet, N.; Doré, M. Formation de chloropicrine en milieu aqueux: Influence des nitrites sur la formation de precurseurs par oxydation de composes organiques. *Water Res.* **1987**, *21* (7), 813−821.
(8) Hu, J.; Song, H.; Karanfil, T. Comparative analysis of halonitromethane and trihalomethane formation and speciation in drinking water: the effects of disinfectants, pH, bromide, and nitrite. *Environ. Sci. Technol.* **2010**, *44* (2), 794−799.
(9) Merlet, N.; Thibaud, H.; Dore, M. Chloropicrin formation during oxidative treatments in the preparation of drinking water. *Sci. Total Environ.* **1985**, *47*, 223−228.
(10) Hoigné, J.; Bader, H. The formation of trichloronitromethane (chloropicrin) and chloroform in a combined ozonation/chlorination treatment of drinking water. *Water Res.* **1988**, *22* (3), 313−319.
(11) McCurry, D. L.; Quay, A. N.; Mitch, W. A. Ozone promotes chloropicrin formation by oxidizing amines to nitro compounds. *Environ. Sci. Technol.* **2016**, *50* (3), 1209−1217.
(12) Shi, J. L.; McCurry, D. L. Transformation of N-Methylamine Drugs during Wastewater Ozonation: Formation of Nitromethane, an Efficient Precursor to Halonitromethanes. *Environ. Sci. Technol.* **2020**, *54* (4), 2182−2191.
(13) Shi, J. L.; Plata, S. L.; Kleimans, M.; Childress, A. E.; McCurry, D. L. Formation and Fate of Nitromethane in Ozone-Based Water Reuse Processes. *Environ. Sci. Technol.* **2021**, *55* (9), 6281−6289.
(14) LeChevallier, M. W. The case for maintaining a disinfectant residual. *J.-Am. Water Works Assoc.* **1999**, *91* (1), 86−94.
(15) Hua, G.; Reckhow, D. A. Comparison of disinfection byproduct formation from chlorine and alternative disinfectants. *Water Res.* **2007**, *41* (8), 1667−78.
(16) Sedlak, D. L.; von Gunten, U. The chlorine dilemma. *Science* **2011**, *331* (6013), 42−43.
(17) Seidel, C. J.; McGuire, M. J.; Summers, R. S.; Via, S. Have utilities switched to chloramines? *J.-Am. Water Works Assoc.* **2005**, *97* (10), 87−97.
(18) Wolfe, R. L.; Ward, N. R.; Olson, B. H. Inorganic chloramines as drinking water disinfectants: a review. *J.-Am. Water Works Assoc.* **1984**, *76* (5), 74−88.
(19) Wahman, D. G.; Pressman, J. G. Distribution system residuals—is "detectable" still acceptable for chloramines? *J.-Am. Water Works Assoc.* **2015**, *107* (8), 53−63.
(20) Huang, K.; Reber, K. P.; Toomey, M. D.; Haflich, H.; Howarter, J. A.; Shah, A. D. Reactivity of the polyamide membrane monomer with free chlorine: reaction kinetics, mechanisms, and the role of chloride. *Environ. Sci. Technol.* **2019**, *53* (14), 8167−8176.
(21) Glater, J.; Hong, S.-k.; Elimelech, M. The search for a chlorine-resistant reverse osmosis membrane. *Desalination* **1994**, *95* (3), 325−345.
(22) Elimelech, M.; Phillip, W. A. The future of seawater desalination: energy, technology, and the environment. *Science* **2011**, *333* (6043), 712−717.
(23) Furst, K. E.; Pecson, B. M.; Webber, B. D.; Mitch, W. A. Distributed chlorine injection to minimize NDMA formation during chloramination of wastewater. *Environ. Sci. Technol. Lett.* **2018**, *5* (7), 462−466.
(24) Mitch, W. A.; Oelker, G. L.; Hawley, E. L.; Deeb, R. A.; Sedlak, D. L. Minimization of NDMA formation during chlorine disinfection of municipal wastewater by application of pre-formed chloramines. *Environ. Eng. Sci.* **2005**, *22* (6), 882−890.
(25) Copeland, A.; Lytle, D. A. Measuring the oxidation−reduction potential of important oxidants in drinking water. *J.-Am. Water Works Assoc.* **2014**, *106* (1), E10−E20.
(26) Chamberlain, E.; Adams, C. Oxidation of sulfonamides, macrolides, and carbadox with free chlorine and monochloramine. *Water Res.* **2006**, *40* (13), 2517−2526.
(27) Orvik, J. A. Kinetics and mechanism of nitromethane chlorination. A new rate expression. *J. Am. Chem. Soc.* **1980**, *102* (2), 740−743.
(28) Pearson, R. G.; Dillon, R. L. Rates of ionization of pseudo acids. 1 IV. relation between rates and equilibria. *J.-Am. Water Works Assoc.* **1953**, *75* (10), 2439−2443.
(29) Heasley, V. L.; Fisher, A. M.; Herman, E. E.; Jacobsen, F. E.; Miller, E. W.; Ramirez, A. M.; Royer, N. R.; Whisenand, J. M.; Zoetewey, D. L.; Shellhamer, D. F. Investigations of the reactions of monochloramine and dichloramine with selected phenols: Examination of humic acid models and water contaminants. *Environ. Sci. Technol.* **2004**, *38* (19), 5022−5029.
(30) Rule, K. L.; Ebbett, V. R.; Vikesland, P. J. Formation of chloroform and chlorinated organics by free-chlorine-mediated oxidation of triclosan. *Environ. Sci. Technol.* **2005**, *39* (9), 3176−3185.
(31) Greyshock, A. E.; Vikesland, P. J. Triclosan reactivity in chloraminated waters. *Environ. Sci. Technol.* **2006**, *40* (8), 2615−2622.
(32) Chuang, Y.-H.; McCurry, D. L.; Tung, H.-h.; Mitch, W. A. Formation pathways and trade-offs between haloacetamides and haloacetaldehydes during combined chlorination and chloramination of lignin phenols and natural waters. *Environ. Sci. Technol.* **2015**, *49* (24), 14432−14440.
(33) Nielsen, A. *The Chemistry of the Nitro and Nitroso Groups. Part 1*; 1969; p 423.
(34) Feng, Y.; Smith, D. W.; Bolton, J. R. Photolysis of aqueous free chlorine species (HOCl and OCl) with 254 nm ultraviolet light. *J.Environ. Eng. Sci.* **2007**, *6* (3), 277−284.
(35) Schreiber, I. M.; Mitch, W. A. Influence of the order of reagent addition on NDMA formation during chloramination. *Environ. Sci. Technol.* **2005**, *39* (10), 3811−3818.
(36) Cavanagh, J. E.; Weinberg, H. S.; Gold, A.; Sangaiah, R.; Marbury, D.; Glaze, W. H.; Collette, T. W.; Richardson, S. D.; Thruston, A. D., Jr Ozonation byproducts: identification of bromohydrins from the ozonation of natural waters with enhanced bromide levels. *Environ. Sci. Technol.* **1992**, *26* (8), 1658−1662.
(37) McCurry, D. L.; Bear, S. E.; Bae, J.; Sedlak, D. L.; McCarty, P. L.; Mitch, W. A. Superior removal of disinfection byproduct precursors and pharmaceuticals from wastewater in a staged anaerobic fluidized membrane bioreactor compared to activated sludge. *Environ. Sci. Technol. Lett.* **2014**, *1* (11), 459−464.
(38) Li, Y.; Kemper, J. M.; Datuin, G.; Akey, A.; Mitch, W. A.; Luthy, R. G. Reductive dehalogenation of disinfection byproducts by an activated carbon-based electrode system. *Water Res.* **2016**, *98*, 354−362.
(39) Allen, J. M.; Cuthbertson, A. A.; Liberatore, H. K.; Kimura, S. Y.; Mantha, A.; Edwards, M. A.; Richardson, S. D. Showering in Flint, MI: Is there a DBP problem? *J. Environ. Sci.* **2017**, *58*, 271−284.
(40) Furst, K. E.; Coyte, R. M.; Wood, M.; Vengosh, A.; Mitch, W. A. Disinfection byproducts in Rajasthan, India: are trihalomethanes a sufficient indicator of disinfection byproduct exposure in low-income countries? *Environ. Sci. Technol.* **2019**, *53* (20), 12007−12017.
(41) Kahler, A. M.; Cromeans, T. L.; Roberts, J. M.; Hill, V. R. Source water quality effects on monochloramine inactivation of adenovirus, coxsackievirus, echovirus, and murine norovirus. *Water Res.* **2011**, *45* (4), 1745−1751.
(42) Kimura, S. Y.; Komaki, Y.; Plewa, M. J.; Mariñas, B. J. Chloroacetonitrile and N, 2-dichloroacetamide formation from the reaction of chloroacetaldehyde and monochloramine in water. *Environ. Sci. Technol.* **2013**, *47* (21), 12382−12390.
(43) Vu, T. N.; Kimura, S. Y.; Plewa, M. J.; Richardson, S. D.; Mariñas, B. J. Predominant N-haloacetamide and haloacetonitrile formation in drinking water via the aldehyde reaction pathway. *Environ. Sci. Technol.* **2019**, *53* (2), 850−859.
(44) Hossain, S.; Chow, C. W.; Cook, D.; Sawade, E.; Hewa, G. A. Review of chloramine decay models in drinking water system. *Environ. Sci.: Water Res. Technol.* **2022**, *8* (5), 926−948.

https://doi.org/10.1021/acs.est.2c09821
Environ. Sci. Technol. XXXX, XXX, XXX−XXX

(45) Zhang, W.; DiGiano, F. A. Comparison of bacterial regrowth in distribution systems using free chlorine and chloramine: a statistical study of causative factors. *Water Res.* **2002**, *36* (6), 1469−1482.
(46) Nguyen, C.; Elfland, C.; Edwards, M. Impact of advanced water conservation features and new copper pipe on rapid chloramine decay and microbial regrowth. *Water Res.* **2012**, *46* (3), 611−621.
(47) Wahman, D. G.; Speitel, G. E., Jr Relative importance of nitrite oxidation by hypochlorous acid under chloramination conditions. *Environ. Sci. Technol.* **2012**, *46* (11), 6056−6064.
(48) Valentine, R. L.; Jafvert, C. T. General acid catalysis of monochloramine disproportionation. *Environ. Sci. Technol.* **1988**, *22* (6), 691−696.
(49) Ianni, J. *Kintecus*, ver. 3.0, Windows Version; 2002 (http://www.kintecus.com).
(50) Jafvert, C. T.; Valentine, R. L. Reaction scheme for the chlorination of ammoniacal water. *Environ. Sci. Technol.* **1992**, *26* (3), 577−586.
(51) McCurry, D. L.; Ishida, K. P.; Oelker, G. L.; Mitch, W. A. Reverse Osmosis Shifts Chloramine Speciation Causing Re-Formation of NDMA during Potable Reuse of Wastewater. *Environ. Sci. Technol.* **2017**, *51* (15), 8589−8596.
(52) Huang, M. E.; Huang, S.; McCurry, D. L. Re-examining the role of dichloramine in high-yield N-Nitrosodimethylamine formation from N, N-Dimethyl-α-arylamines. *Environ. Sci. Technol. Lett.* **2018**, *5* (3), 154−159.
(53) Aiken, F.; Cox, B. G.; Sørensen, P. E. Proton transfer from carbon. A study of the acid−base-catalysed relaxation and the bromination of aryl-substituted methanedisulfones. *J. Chem. Soc., Perkin Trans.2* **1993**, No. 4, 783−790.
(54) Beal, L. D.; Hill, D. C.; Martin, R. A.; Hedengren, J. D. Gekko optimization suite. *Processes* **2018**, *6* (8), 106.
(55) Lim, S.; Shi, J. L.; von Gunten, U.; McCurry, D. L. Ozonation of Organic Compounds in Water and Wastewater: A Critical Review. *Water Res.* **2022**, *213*, 118053.
(56) Leskovac, V. Kinetic Isotope Effects. *Comprehensive Enzyme Kinetics* **2003**, 353−390.
(57) Anslyn, E. V.; Dougherty, D. A. *Modern physical organic chemistry*; University Science Books: Sausalito, CA, 2006.
(58) Wynne-Jones, W. Acid-base reactions involving deuterium. *J. Chem. Phys.* **1934**, *2* (7), 381−385.
(59) Bordwell, F.; Boyle, W. J., Jr Kinetic isotope effects for nitroalkanes and their relation to transition-state structure in proton-transfer reactions. *J. Am. Chem. Soc.* **1975**, *97* (12), 3447−3452.
(60) Salomaa, P.; Schaleger, L. L.; Long, F. Solvent deuterium isotope effects on acid-base equilibria. *J. Am. Chem. Soc.* **1964**, *86* (1), 1−7.
(61) Bell, R. P.; Goodall, D. M. Kinetic hydrogen isotope effects in the ionization of some nitroparaffins. *Proc. R. Soc. A* **1966**, *294* (1438), 273−297.
(62) Chuang, Y.-H.; Tung, H.-h. Formation of trichloronitromethane and dichloroacetonitrile in natural waters: precursor characterization, kinetics and interpretation. *J. Hazard. Mater.* **2015**, *283*, 218−226.
(63) Nihemaiti, M.; Le Roux, J.; Hoppe-Jones, C.; Reckhow, D. A.; Croué, J.-P. Formation of haloacetonitriles, haloacetamides, and nitrogenous heterocyclic byproducts by chloramination of phenolic compounds. *Environ. Sci. Technol.* **2017**, *51* (1), 655−663.
(64) Lau, S. S.; Dias, R. P.; Martin-Culet, K. R.; Race, N. A.; Schammel, M. H.; Reber, K. P.; Roberts, A. L.; Sivey, J. D. 1, 3, 5-Trimethoxybenzene (TMB) as a new quencher for preserving redox-labile disinfection byproducts and for quantifying free chlorine and free bromine. *Environ. Sci.: Water Res. Technol.* **2018**, *4* (7), 926−941.
(65) Bunting, J. W.; Stefanidis, D. A systematic entropy relationship for the general-base catalysis of the deprotonation of a carbon acid. A quantitative probe of transition-state solvation. *J. Am. Chem. Soc.* **1990**, *112* (2), 779−786.
(66) Cope, S. M.; Tailor, D.; Nagorski, R. W. Determination of the p K a of Cyclobutanone: Brønsted Correlation of the General Base-Catalyzed Enolization in Aqueous Solution and the Effect of Ring Strain. *J. Org. Chem.* **2011**, *76* (2), 380−390.
(67) Toth, K.; Richard, J. P. Covalent catalysis by pyridoxal: evaluation of the effect of the cofactor on the carbon acidity of glycine. *J. Am. Chem. Soc.* **2007**, *129* (10), 3013−3021.
(68) Duirk, S. E.; Desetto, L. M.; Davis, G. M.; Lindell, C.; Cornelison, C. T. Chloramination of organophosphorus pesticides found in drinking water sources. *Water Res.* **2010**, *44* (3), 761−768.
(69) Gerrity, D.; Pecson, B.; Trussell, R. S.; Trussell, R. R. Potable reuse treatment trains throughout the world. *J. Water Supply: Res. Technol.–Aqua* **2013**, *62* (6), 321−338.

https://doi.org/10.1021/acs.est.2c09821
Environ. Sci. Technol. XXXX, XXX, XXX−XXX